Simulation of ozone loss in Arctic winter 2004/05

J.-U. Grooß and R. Müller

Institut für Chemie und Dynamik der Geosphäre, ICG-1: Stratosphäre, Forschungszentrum Jülich, Germany

Accepted for publication in Geophysical Reserch Letters.

Short title: OZONE LOSS IN ARCTIC WINTER 2004/05

Abstract. We present simulations of stratospheric ozone depletion in the Arctic winter 2004/05 by the Chemical Lagrangian Model of the Stratosphere (CLaMS). This winter is among the coldest on record with large observed ozone losses. It is also different from previously analyzed winters, as ozone mixing ratios within the polar vortex were not homogeneously distributed. The reason for the untypical ozone distribution is a second transport barrier that existed at the time of vortex formation. The simulations agree well with ozone measurements by the Fourier Transform Spectrometer (ACE-FTS). The simulated vortex average column ozone loss between 380 and 550 K potential temperature ($\pm 1\sigma$) was 69 ± 21 Dobson Units on 23 March. The simulated ozone loss is in approximate agreement with some published estimates, but is significantly lower than others. A possible reason for this difference is the inhomogeneous ozone distribution within the vortex which makes it more complicated to estimate of ozone loss.

Introduction

Chemical ozone depletion in the polar stratosphere is a phenomenon that has been investigated for about two decades. It is now well accepted that polar ozone depletion is caused by anthropogenic halogen emissions and that it is closely linked to low stratospheric temperatures [e.g. *WMO*, 2003]. Here we investigate the Arctic stratospheric winter 2004/05, which is among the coldest Arctic winters on record [*Rex et al.*, 2006] using simulations of the Chemical Lagrangian Model of the Stratosphere (CLaMS) [*McKenna et al.*, 2002a, b]. Ozone loss in this winter was previously estimated by using a variety of methods and data sources. In the following, we compare our simulation with those estimates.

Rex et al. [2006] use ozone sonde observations to diagnose ozone loss by the so-called vortex average method. They report significant ozone loss. In particular, the ozone loss below 400 K is significantly larger than in previous years. *Manney et al.* [2006] diagnose ozone loss from EOS-MLS and POAM data. They show formation of a low ozone vortex core and evidence of mixing at the vortex edge from N_2O data. *Jin et al.* [2006] present estimates of ozone loss between early January to mid-March from ACE-FTS data using various methods: the tracer correlation method with CH_4, the tracer correlation method with an artificial tracer, and the vortex average method.

Both *Manney et al.* [2006] and *Jin et al.* [2006] highlight the difficulty in diagnosing ozone loss, especially in winter 2004/05, due to mixing in the vortex edge region and the inhomogeneous ozone distribution within the vortex which may increase the uncertainty of the deduced ozone loss. They state the need for detailed simulations to interpret the ozone loss in

this winter. *Singleton et al.* [2006] estimate chemical ozone loss from the difference between passive ozone simulated by the SLIMCAT chemical transport model and ozone measured by various instruments (POAM III, SAGE III, MLS, ACE-FTS, MAESTRO).

Moreover, *Dufour et al.* [2006] report strong chlorine activation until early March on the basis of ACE-FTS data. *Von Hobe et al.* [2006] show in-situ observations of almost full chlorine activation on March 7. They also show that the observations are comparable with the simulation presented here and estimate column ozone loss for the location of the flight in the vortex core. Here we present CLaMS simulations that aim to reproduce both mixing and chemical ozone loss in detail for the challenging conditions of this winter.

CLaMS Simulation

The Chemical Lagrangian Model of the Stratosphere (CLaMS) is a Lagrangian 3-dimensional chemical transport model which is described elsewhere [*McKenna et al.*, 2002a, b; *Konopka et al.*, 2004; *Grooß et al.*, 2005]. Here we present CLaMS simulations for the Northern hemisphere with a horizontal resolution of 100 km/300 km north/south of 40°N, respectively. As the air parcels are distributed irregularly in space, the resolution is defined by the mean distance of neighboring air parcels. The vertical coordinate is the potential temperature with 32 levels between 320 and 900 K corresponding to a vertical resolution of about 0.4 km. Vertical motion is calculated as the time derivative of the potential temperature using a radiation scheme [*Morcrette*, 1991]. Mixing is simulated at those locations where strong wind shear occurs using the Lagrangian mixing algorithm [*McKenna et al.*, 2002a; *Konopka et al.*, 2004]. Heterogeneous chemistry on water ice, nitric acid trihydrate (NAT),

and liquid ternary $H_2O/HNO_3/H_2SO_4$ solution (STS) particles is included. The nucleation of NAT from STS requires a supersaturation of HNO_3 over NAT of 30 and is therefore strongly hindered. The four particle types may coexist in the steady state. Further details are presented by *McKenna et al.* [2002b]. Sedimentation of NAT particles was calculated as in *Grooß et al.* [2005] using a globally constant nucleation rate of $8{\cdot}10^{-6}\,\mathrm{cm}^{-3}\mathrm{h}^{-1}$ in regions where temperatures are below the NAT equilibrium temperature T_{NAT}.

The initialization of chemical species on 20 November 2004 was derived from AURA-MLS O_3 and N_2O data (version 1.51) [*Manney et al.*, 2006] and ACE-FTS O_3 data (version 2.2 update) [*Walker et al.*, 2005]. Using the CLaMS trajectory module, all MLS observations between 18 and 23 November were mapped to the synoptic time 20 November 12:00 UT onto a regular $2^\circ \times 6^\circ$ grid using a cosine-square distance weighting. An offset between AURA-MLS and ACE-FTS O_3 data was found, as also reported by *Singleton et al.* [2006]. The O_3 initialization was therefore corrected by the following empirical fit derived from ACE data between 20 November and 5 December and an MLS-initialized CLaMS simulation:

$$\mathrm{O}_3^{\mathrm{corr}} = \mathrm{O}_3^{\mathrm{MLS}} + 0.6734 - 0.001528 \cdot \theta,$$

where O_3 is given in ppmv and the potential temperature is in the range $375\,\mathrm{K} < \theta < 775\,\mathrm{K}$. The initialization is then consistent with the ACE-FTS data. The other chemical tracers and families CH_4, Cl_y, and Br_y were initialized using the N_2O/CH_4, CH_4/Cl_y and CH_4/Br_y relations as for the 2002/03 winter [*Grooß et al.*, 2005]. The remaining chemical species were taken from the Mainz 2-D model [*Gidel et al.*, 1983; *Grooß*, 1996] mapped to equivalent

latitude (Φ_e). Reaction rate constants and absorption cross sections were taken from standard recommendations [*Sander et al.*, 2003].

The boundary conditions prescribed at the upper model boundary (900 K) were derived by the same method as for the initialization. MLS data and 2-D model output and the above-mentioned correlations were combined in the same way for every half month. As the predominant vertical velocity in the vortex is downward, the lower boundary (320 K) was not forced to any external value. Ozone loss and denitrification in the simulation are calculated by taking the difference between simulations O_3 and NO_y with passive tracers O_3^{pass} and NO_y^* that are advected and mixed but undergo no chemical change. These passive tracers were initialized on 20 November 2004 as O_3 and NO_y, respectively.

Results

The first results of this CLaMS simulation were presented in comparison with in-situ observations by *von Hobe et al.* [2006]. They show observations of strong chlorine activation on 7 March 2005 in agreement with the CLaMS simulation that can only be explained if a significant denitrification (about 70%) has also been simulated. The maximum denitrification averaged over the vortex (poleward of 65° equivalent latitude) is 8.1 ppbv (corresponding to 50% of NO_y^*), which is reached on the 485 K level on 27 January. Denitrification is stronger in the vortex core. *Grooß et al.* [2005] have shown that the effect of denitrification on ozone loss is moderate (7% of the column ozone loss between 380 and 550 K in 2003).

The focus of this study is the CLaMS simulation of ozone and of ozone loss. Figure 1 shows the simulated ozone mixing ratio on the 475 K potential temperature level averaged

over 40 equivalent latitude bins between 40° and 90°N, where each bin contains an equal area (bin size 0.78° at Φ_e=65°). The black line corresponds to the vortex edge after *Nash et al.* [1996]. Unlike in earlier winters, ozone within the polar vortex is obviously not distributed homogeneously from the beginning of the winter onwards. This inhomogeneity is noticeable in observations by EOS-MLS [*Manney et al.*, 2006; *von Hobe et al.*, 2006] and ozone sondes [*Rex et al.*, 2006].

In order to validate the simulated ozone mixing ratios, we first compare them with satellite observations of ACE-FTS (version 2.2 update) [*Walker et al.*, 2005]. To this end, the CLaMS results were interpolated to the exact observation location and time, where the displacement between 12:00 UT (CLaMS output time) and the observation time was taken into account by trajectory calculations. Figure 2 shows this comparison for 3 different time intervals, one in early winter (1 to 14 January) before significant ozone depletion has occurred, and two at the end of the winter (1 to 8 March and 12 to 25 March) for equivalent latitudes Φ_e poleward of 65°. All points lie close to the 1:1 line. The largest deviations occur for low equivalent latitudes, that means for locations close to the vortex edge. All the time intervals shown contain observations at equivalent latitudes between 65° and 87°. The average difference ($\pm 1\sigma$ standard deviation) between observations and simulations ($\Phi_e > 65°$N, CLaMS-FTS) are 0.03 ± 0.33 ppmv, 0.00 ± 0.30 ppmv and -0.04 ± 0.32 ppmv, respectively, for these three time intervals. Thus the simulation is in excellent agreement with the observations, which means that the model reproduces the observed inhomogeneity of the ozone distribution within the vortex. This implies that the simulation should also allow ozone loss to be estimated with high accuracy.

The reason for this untypical ozone distribution is a second transport barrier during the formation of the polar vortex. The vortex edge determined according to the method of *Nash et al.* [1996] (black line in Figure 1) frequently switches between around 65° and around 75° during December because the two transport barriers are of similar strength at this time. To illustrate this point, Figure 3 shows the development of the two transport barriers in winter 2004/05. These are determined as d(PV)/dΦ_e from ECMWF analyses in $1^\circ \times 1^\circ$ resolution. A significant transport barrier at about 75° equivalent latitude already develops in October and hinders the poleward flow of ozone-rich mid-latitude air during the formation period of the vortex. Similar double transport barriers have been reported for the southern hemisphere [*Lee et al.*, 2001; *Tilmes et al.*, 2006]. Such double transport barriers for the formation period of the polar vortex have not been reported hitherto for Arctic winters. From late December throughout mid-March, the outer transport barrier is stronger and therefore identified as the vortex edge by the method of *Nash et al.* [1996]. However, from early February to mid-March, the inner transport barrier corresponds most of the time to values of $d\mathrm{PV}/d\Phi_e$ above 0.5 PVU/degree, corresponding to a moderate isolation of the vortex core air masses from the vortex edge region.

In the following, the simulated ozone loss is presented in detail. Figure 4a shows the vortex average (equivalent latitude Φ_e >65°N) accumulated ozone loss versus time and potential temperature. This was determined as the difference between simulated ozone and the passive ozone tracer O_3^{pass}. The simulated average ozone loss ($\pm 1\sigma$ variability) maximizes at 1.4 ± 0.3 ppmv on the 475 K level on March 19 (corresponding to 38% of O_3^{pass}). Also visible is the ozone depletion above about 550 K that is caused by catalytic cycles involving NO_x

similar to the situation in earlier winters [*Grooß et al.*, 2005; *Konopka et al.*, 2006]. Figure 4b shows the ozone loss on the 475 K level averaged over equivalent latitude bins (corresponding to Figure 1). The peak ozone loss in this view is 1.6 ppmv between 80° and 90° equivalent latitude on March 25. Figure 4c shows the column ozone loss between 380 and 550 K potential temperature. Unlike ozone itself, the chemical ozone loss does not show a strong correlation with equivalent latitude. Here, the column was calculated by first calculating vortex average ozone loss on the different theta levels and then performing a vertical integrating using vortex average temperature profiles. Due to the availability of sunlight, the ozone loss in January is slightly stronger towards the vortex edge. Because of the higher chlorine activation in the vortex core, in March more ozone loss is simulated towards the vortex core. The simulated partial column ozone loss between potential temperatures of 380 and 550 K averaged over the area poleward of Φ_e=65° ($\pm 1\sigma$ variability) reaches its largest value of 69$\pm$21 DU on 23 March. In the vortex core ($\Phi_e \geq 75°$) the maximum partial column ozone loss is 77$\pm$15 DU.

The ozone depletion reported here is lower than most other published ozone loss estimates for this winter. *Jin et al.* [2006] calculate the vortex ozone loss using different tracer correlations for ACE-FTS data and estimate between 1.8 to 2.3 ppmv at 475-500 K depending on the method. The corresponding column ozone loss ranges from 116 to 127 DU. At least part of the discrepancy between their estimates and our model results is caused by the fact that they do not take into account the varying latitudinal coverage of ACE-FTS. They chose a reference period from 1 to 7 January and compare this with observations from 8 to 15 March. While the latitude of the reference observations is close to the vortex edge (average equivalent latitude $\pm 1\sigma$ of 70.5$\pm$5°), the March observations are located further towards the vortex core

(74±5°). Due to the inhomogeneous ozone distribution (see Figure 1), calculating the ozone loss as the ozone difference of these two regions should result in an overestimation of ozone depletion.

The CLaMS ozone loss estimate is closer to that of *Singleton et al.* [2006], who show the difference between various data sets and a passive ozone simulation. The vortex average ozone loss partial column between 400 and 575 K using the ACE-FTS data is about 100 DU in mid-March (Figure 8 from *Singleton et al.* [2006]). From this value, the initial ozone offset of about 10-20 DU must be subtracted resulting in about 85 DU chemical ozone loss. The corresponding CLaMS ozone loss between 400 and 575 K in mid-March is 69, 74, and 76 DU poleward of 65°, 70°, and 75° equivalent latitude, respectively.

The estimated ozone depletion reported here is also significantly lower than the estimates of *Rex et al.* [2006] (1.7 ppmv at 425 K, 121±20 DU partial column 380-550 K). The reason for the significantly larger ozone loss estimates compared to this study (69±21 DU) is unclear at present.

Von Hobe et al. [2006] estimate column ozone loss to be 62^{+8}_{-17} DU between 344 and 460 K in the vortex core. There are larger uncertainties of the tracer correlation in the lowest part of the observed profile and also the model results close to the lower model boundary may be somewhat more uncertain. For comparison with CLaMS, we therefore re-evaluate the ozone column loss from the Geophysica measurements for the vertical range between 380 and 460 K to be 39^{+6}_{-11} DU. The corresponding CLaMS ozone column evaluated at the flight location is 27 DU. Most of the difference (10 DU) is due to the difference in passive ozone. About 2 DU of the difference is due to a slight overestimate of observed ozone by the

simulation. As in the comparison with *Jin et al.* [2006], the observed air masses do rather show the vortex core characteristic and therefore the lower estimate of *von Hobe et al.* [2006], which is derived from the vortex core reference relation, is more realistic.

The simulated ozone depletion is comparable with the estimations of *Manney et al.* [2006], who diagnose a vortex average ozone loss of 1.2-1.5 ppmv between 450 and 500 K on March 10 from EOS-MLS data. This is in agreement with CLaMS, which has a vortex average ozone loss peak of 1.37 ppmv (± 0.29ppmv) at 475 K potential temperature. *Manney et al.* [2006] also suggest significantly larger ozone loss of up to 2 ppmv in the vortex edge region that is not confirmed by CLaMS, but they also mention the difficulty introduced by the mixing of air into the polar vortex.

Conclusions

The Chemical Lagrangian Model of the Stratosphere (CLaMS) successfully simulated ozone loss in the winter 2004/05. The simulated ozone mixing ratio in the polar vortex is in excellent agreement with the observations of ACE-FTS. The distribution of ozone mixing ratios within the polar vortex in this winter is rather inhomogeneous with lower ozone mixing ratios in the vortex core throughout the winter. This is due to a second transport barrier at about 75° equivalent latitude during the setup phase of the polar vortex. A moderate inner transport barrier is also present from early February to mid-March. The simulation suggests the column ozone depletion (380–550 K) averaged over the polar vortex (equivalent latitudes $\Phi_e > 65°$) reaches its maximum of 69 ± 21 DU on 23 March.

Published ozone loss estimates for this winter vary significantly because some of the

methods assume that the ozone distribution within the vortex is homogeneous. The error estimates accompanying these previous results would be larger if the inhomogeneity of the ozone distribution were considered. The simulated vortex average ozone loss presented here is comparable with the estimates of *Manney et al.* [2006] and *Singleton et al.* [2006] and lower than the estimates of *Rex et al.* [2006], *Jin et al.* [2006] and *von Hobe et al.* [2006]. At least part of the differences from the latter studies may be explained by the exceptionally inhomogeneous ozone distribution within the polar vortex.

Acknowledgments. We thank the scientific teams of MLS and ACE-FTS for the data and useful discussions. The Atmospheric Chemistry Experiment (ACE), also known as SCISAT, is mainly supported by the Canadian Space Agency. ACE-FTS data were kindly provided by ESA-ESRIN as Third Party Mission (TPM) data. The European Centre for Medium-Range Weather Forecasts (ECMWF) provided the meteorological analyses. We thank the CLaMS team at ICG-1 of Forschungszentrum Jülich for excellent support. Thanks are especially due to Nicole Thomas and Barbara Deutsch. We thank Marc von Hobe for fruitful discussions. Simulations were performed on the Jülich Multiprocessor (JUMP) and supported by the John von Neumann-Institute for Computing (NIC).

References

Dufour, G., et al., Partitioning between the inorganic chlorine reservoirs HCl and $ClONO_2$ during the Arctic winter 2005 from the ACE-FTS, *Atmos. Chem. Phys.*, *6*, 2355–2366, 2006.

Gidel, L. T., P. J. Crutzen, and J. Fishman, A two-dimensional photochemical model of the atmosphere; 1: Chlorocarbon emissions and their effect on stratospheric ozone, *J. Geophys. Res.*, *88*, 6622–6640, 1983.

Grooß, J.-U., Modelling of stratospheric chemistry based on HALOE/UARS satellite data, PhD thesis, University of Mainz, 1996.

Grooß, J.-U., G. Günther, R. Müller, P. Konopka, S. Bausch, H. Schlager, C. Voigt, C. M. Volk, and G. C. Toon, Simulation of denitrification and ozone loss for the Arctic winter 2002/2003, *Atmos. Chem. Phys.*, *5*, 1437–1448, 2005.

Jin, J. J., et al., Severe Arctic ozone loss in the winter 2004/2005: observations from ACE-FTS, *Geophys. Res. Lett.*, *33*, L15801, doi:10.1029/2006GL026752, 2006.

Konopka, P., et al., Mixing and ozone loss in the 1999-2000 Arctic vortex: Simulations with the 3-dimensional Chemical Lagrangian Model of the Stratosphere (CLaMS), *J. Geophys. Res.*, *109*, D02315, doi:10.1029/2003JD003792, 2004.

Konopka, P., et al., Ozone loss driven by nitrogen oxides and triggered by stratospheric warmings may outweigh the effect of halogens, *J. Geophys. Res.*, in press, 2006.

Lee, A., H. Roscoe, A. Jones, P. Haynes, E. Shuckburgh, M. Morrey, and H. Pumphrey, The

impact of the mixing properties within the Antarctic stratospheric vortex on ozone loss in spring,, *J. Geophys. Res.*, *106*, 3203–3211, doi:10.1029/2000JD900398, 2001.

Manney, G., M. Santee, L. Froidevaux, K. Hoppel, N. Livesey, and J. Waters, EOS MLS observations of ozone loss in the 2004-2005 Arctic winter, *Geophys. Res. Lett.*, *33*, L04802, doi:10.1029/2005GL024494, 2006.

McKenna, D. S., P. Konopka, J.-U. Grooß, G. Günther, R. Müller, R. Spang, D. Offermann, and Y. Orsolini, A new Chemical Lagrangian Model of the Stratosphere (CLaMS): 1. Formulation of advection and mixing, *J. Geophys. Res.*, *107*(D16), 4309, doi:10.1029/2000JD000114, 2002a.

McKenna, D. S., J.-U. Grooß, G. Günther, P. Konopka, R. Müller, G. Carver, and Y. Sasano, A new Chemical Lagrangian Model of the Stratosphere (CLaMS): 2. Formulation of chemistry scheme and initialization, *J. Geophys. Res.*, *107*(D15), 4256, doi:10.1029/2000JD000113, 2002b.

Morcrette, J.-J., Radiation and cloud radiative properties in the European Centre for Medium-Range Weather Forecasts forecasting system, *J. Geophys. Res.*, *96*(D5), 9121–9132, 1991.

Nash, E. R., P. A. Newman, J. E. Rosenfield, and M. R. Schoeberl, An objective determination of the polar vortex using Ertel's potential vorticity, *J. Geophys. Res.*, *101*, 9471–9478, 1996.

Rex, M., et al., Arctic winter 2005: Implications for stratospheric ozone loss and climate change, *Geophys. Res. Lett.*, *33*, L23808, doi:10.1029/2006GL026731, 2006.

Sander, S. P., et al., *Evaluation number 14*, Chemical kinetics and photochemical data for use in atmospheric studies, NASA Panel for Data Evaluation, JPL Publication 02-25, Jet Propulsion Laboratory, California Insitute of Technology, Pasadena, California, 2003.

Singleton, C. S., et al., Quantifying Arctic ozone loss during the 2004-2005 winter using satellite observations and a chemical transport model, *J. Geophys. Res.*, in press, 2006.

Tilmes, S., R. Müller, J.-U. Grooß, H. Nakajima, and Y. Sasano, Development of tracer relations and chemical ozone loss during the setup phase of the polar vortex, *J. Geophys. Res.*, *111*, D24S90, doi:10.1029/2005JD006726, 2006.

von Hobe, M., et al., Severe ozone depletion in the cold Arctic winter 2004-05, *Geophys. Res. Lett.*, *13*, L17815, doi:10.1029/2006GL026945, 2006.

Walker, K. A., C. E. Randall, C. R. Trepte, C. D. Boone, and P. F. Bernath, Initial validation comparisons for the Atmospheric Chemistry Experiment (ACE-FTS), *Geophys. Res. Lett.*, *32*, L16S04, doi:10.1029/2005GL022388, 2005.

WMO, *Scientific assessment of ozone depletion: 2002*, Report No. 47, Geneva, Switzerland, 2003.

J.-U. Grooß and R. Müller, Institut für Chemie und Dynamik der Geosphäre, ICG-1: Stratosphäre, Forschungszentrum Jülich, 52425 Jülich, Germany (j.-u.grooss@fz-juelich.de)

Received _____

Figure Captions

Figure 1. Simulated development of ozone mixing ratio on the 475 K potential temperature level as averages over equivalent latitude bins. The black line corresponds to the vortex edge after *Nash et al.* [1996]. It is not continuous in December as explained in the text.

Figure 2. Comparison of simulated ozone mixing ratio with observations of ACE-FTS. All observations with equivalent latitude $\Phi_e \geq 65°$N between 350 and 800 K potential temperature are shown. Each panel corresponds to a different time interval indicated in the title. The color of the symbols corresponds to the equivalent latitude of the observation. The equivalent latitude covered in each time interval spans at least 65° to 87°N.

Figure 3. Development of transport barriers on the 475 K potential temperature level. The slope d(PV)/dΦ_e is shown as function of equivalent latitude and time. The black lines correspond to the relative maximum for equivalent latitudes poleward/equatorward of 70° determined after the algorithm of *Nash et al.* [1996] which also considers the wind speed. The lines are 3-day running means, and the linestyle indicates the strength of the transport barrier: dotted and solid lines correspond to d(PV)/dΦ_e larger than 0.3 and 0.5 PVU/degree, respectively.

Figure 4. Development of simulated ozone loss in different representations. The top panel shows the vortex average ozone loss ($\Phi_e > 65°$N) versus time and potential temperature, the middle panel a horizontal cut at 475 K, and the bottom panel the corresponding column ozone loss between 380 and 550 K potential temperature. The black line in the middle and bottom panels corresponds to the vortex edge at 475 K after *Nash et al.* [1996] as in Figure 1.

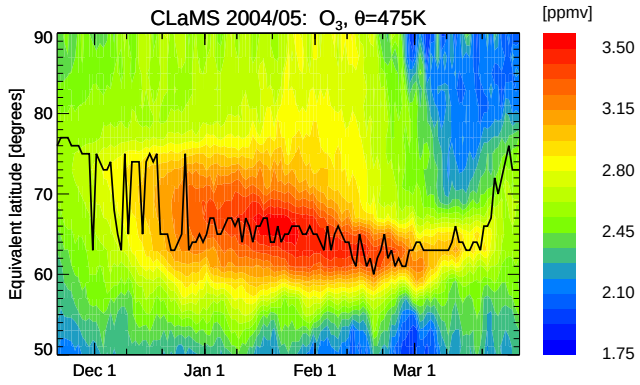
CLaMS 2004/05: O3, θ=475K
[ppmv]
3.50
3.15
2.80
2.45
2.10
1.75
Equivalent latitude [degrees]
90
80
70
60
50
Dec 1
Jan 1
Feb 1
Mar 1

Figure 1.

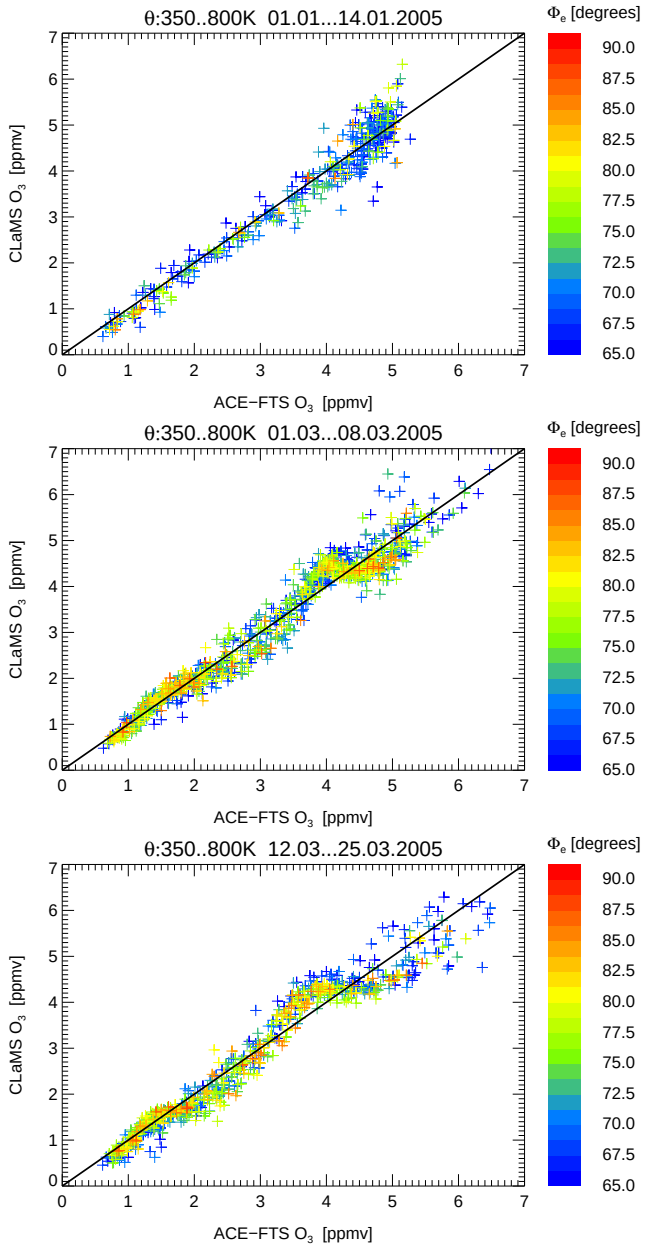
θ:350..800K 01.01...14.01.2005
θ:350..800K 01.03...08.03.2005
θ:350..800K 12.03...25.03.2005
CLaMS O3 [ppmv]
ACE−FTS O3 [ppmv]
Φe [degrees]
90.0
87.5
85.0
82.5
80.0
77.5
75.0
72.5
70.0
67.5
65.0

Figure 2.

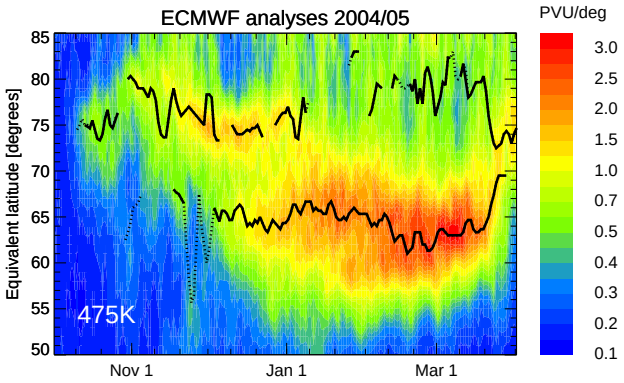
ECMWF analyses 2004/05
PVU/deg
3.0
2.5
2.0
1.5
1.0
0.7
0.5
0.4
0.3
0.2
0.1
Equivalent latitude [degrees]
85
80
75
70
65
60
55
50
475K
Nov 1
Jan 1
Mar 1

Figure 3.

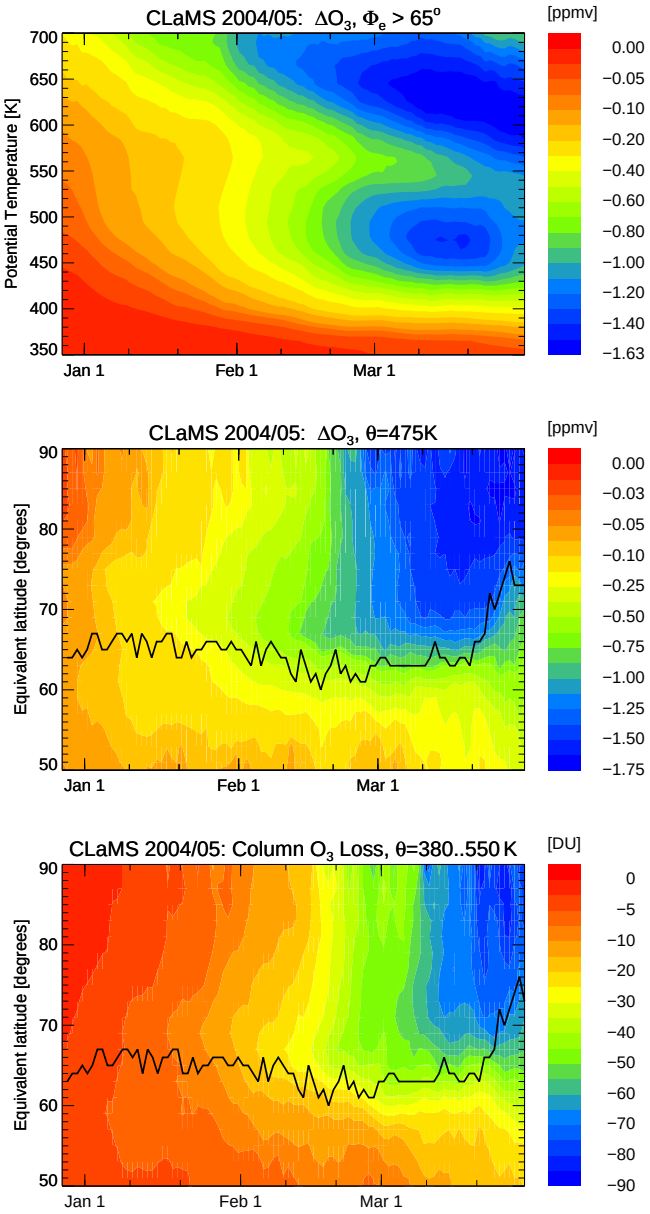
CLaMS 2004/05: ΔO3, Φe > 65°
[ppmv]
Potential Temperature [K]
700
650
600
550
500
450
400
350
Jan 1
Feb 1
Mar 1
0.00
−0.05
−0.10
−0.20
−0.40
−0.60
−0.80
−1.00
−1.20
−1.40
−1.63
CLaMS 2004/05: ΔO3, θ=475K
[ppmv]
Equivalent latitude [degrees]
90
80
70
60
50
Jan 1
Feb 1
Mar 1
0.00
−0.03
−0.05
−0.10
−0.25
−0.50
−0.75
−1.00
−1.25
−1.50
−1.75
CLaMS 2004/05: Column O3 Loss, θ=380..550 K
[DU]
Equivalent latitude [degrees]
90
80
70
60
50
Jan 1
Feb 1
Mar 1
0
−5
−10
−20
−30
−40
−50
−60
−70
−80
−90

Figure 4.